

High Photon Number Entangled States and Coherent State Superposition from the Extreme Ultraviolet to the Far Infrared

Philipp Stammer,^{1,2,*} Javier Rivera-Dean¹, Theocharis Lamprou,^{3,4} Emilio Pisanty^{2,5},

Marcelo F. Ciappina^{6,7}, Paraskevas Tzallas^{3,8} and Maciej Lewenstein^{1,9}

¹*ICFO—Institut de Ciències Fotoniques, The Barcelona Institute of Science and Technology, 08860 Castelldefels (Barcelona), Spain*

²*Max Born Institute for Nonlinear Optics and Short Pulse Spectroscopy, Max Born Strasse 2a, D-12489 Berlin, Germany*

³*Foundation for Research and Technology-Hellas, Institute of Electronic Structure & Laser, GR-70013 Heraklion (Crete), Greece*

⁴*Department of Physics, University of Crete, P.O. Box 2208, GR-70013 Heraklion (Crete), Greece*


⁵*Department of Physics, King's College London, Strand, WC2R 2LS London, United Kingdom*

⁶*Physics Program, Guangdong Technion—Israel Institute of Technology, Shantou, Guangdong 515063, China*

⁷*Technion—Israel Institute of Technology, Haifa 32000, Israel*

⁸*ELI-ALPS, ELI-Hu Non-Profit Ltd., Dugonics tér 13, H-6720 Szeged, Hungary*

⁹*ICREA, Pg. Lluís Companys 23, 08010 Barcelona, Spain*

 (Received 4 August 2021; revised 7 February 2022; accepted 1 March 2022; published 25 March 2022)

We present a theoretical demonstration on the generation of entangled coherent states and of coherent state superpositions, with photon numbers and frequencies orders of magnitude higher than those provided by the current technology. This is achieved by utilizing a quantum mechanical multimode description of the single- and two-color intense laser field driven process of high harmonic generation in atoms. It is found that all field modes involved in the high harmonic generation process are entangled, and upon performing a quantum operation, lead to the generation of high photon number optical cat states spanning from the far infrared to the extreme ultraviolet spectral region. This provides direct insights into the quantum mechanical properties of the optical field in the intense laser matter interaction. Finally, these states can be considered as a new resource for fundamental tests of quantum theory, quantum information processing, or sensing with nonclassical states of light.

DOI: [10.1103/PhysRevLett.128.123603](https://doi.org/10.1103/PhysRevLett.128.123603)

The superposition of classically distinguishable states is of fundamental interest since the development of quantum theory, and was brought to an extreme by Schrödinger in his famous *Gedankenexperiment* [1]. In quantum optics this notion can be retrieved by superpositions of coherent states [2,3]. Besides their use for fundamental testing of quantum mechanics [4,5], the generation of these Schrödinger cat states, and of entangled coherent states [6,7], is also of direct technological importance. These states are a powerful tool in quantum information processing [8–11], quantum computation [12,13], quantum metrology [14], or can be used to visualize the classical-to-quantum transition [15]. To generate superpositions of coherent states, atom-light interaction in cavities [16,17], or conditioning approaches at the output of a beam splitter [18–20] can be employed. Such conditioning experiments are of general interest in quantum information theory due to their ability to generate entangled optical states [21], to describe quantum operations [22] or conditional quantum measurements [23,24]. But, the size of the generated superpositions of coherent states is limited to the range of a few photons, corresponding to moderately small

coherent state amplitudes [3,25,26], restricting their applicability in quantum information processing. However, due to the relevance of such nonclassical states of light in quantum technologies [8,13,27], it is of particular interest to generate a superposition, and entanglement, of coherent states with high photon numbers. In the present Letter we show how both can be achieved by means of a conditioning procedure, performed on a so far unrelated photonic platform, namely, intense laser-matter interaction. Laser sources can easily reach intensities of up to 10^{14} W/cm², and the field induced material response can be highly nonlinear [28]. Since these laser fields naturally involve very high photon numbers with corresponding coherent state amplitudes in the range of $|\alpha| = 10^6$, it will be of great advantage to use them for the generation of the sought high photon number nonclassical field states [29,30]. Until recently the intense laser-matter interaction was mainly described by a semiclassical theory, in which the laser field was considered classically such that the properties of the quantum state of the field were not envisioned. A commonly used intense laser driven process is the generation of high-order harmonics, in which the coherent properties of

the driving laser are transferred to an electronic wave packet, and later returned to the field modes by the emission of coherent radiation at frequencies of integer multiple of the driving laser field [31]. However, recent advances in the quantum optical description of high harmonic generation (HHG) [30,32–36] allow us to conceive new experiments, in which nonclassical properties of the field can be observed with prospective use for modern quantum technologies. In particular, it was shown that a conditioning procedure on HHG can lead to nonclassical optical Schrödinger cat states in the infrared spectral range [30]. To extend the approach to different spectral regions, and to unravel the entanglement between all field modes participating in the HHG process, we have developed a complete quantum mechanical multimode approach. This is used for the description of the interaction of atoms with single- and two-color intense laser fields. We show that all field modes involved in the HHG process are naturally entangled, and upon performing a quantum operation leads to the generation of a high photon number coherent state superposition spanning from the extreme ultraviolet (XUV) to the far infrared (IR). We provide the conditions for the generation of XUV cat states, and for the generation of entangled coherent states between two frequency modes in the IR regime with very high photon numbers.

For the description we consider an uncorrelated state prior to the laser-matter interaction $|g\rangle \otimes |\phi\rangle$, in which the atom is prepared in its ground state $|g\rangle$ and the field is described by $|\phi\rangle = |\alpha\rangle \otimes |\{0_q\}\rangle$, where $|\{0_q\}\rangle = \otimes_q |0_q\rangle$. The intense driving laser in the fundamental mode is in a coherent state $|\alpha\rangle$, and the harmonic modes $q \in \{2, \dots, N\}$ are in the vacuum, where the generated harmonics extend to a cutoff N . If the interaction is conditioned on the atomic ground state (leading to HHG) [30,31], neglecting the correlations of the atomic dipole moment [37], the effective interaction is described by a multimode displacement operator [30,38], $D(\chi) = \prod_{q=1}^N D(\chi_q)$, where $\chi_q = -i\kappa\sqrt{q}\langle d \rangle(q\omega)$, with coupling constant κ , and the Fourier transform of the time-dependent dipole moment expectation value $\langle d \rangle(q\omega) = \int_{-\infty}^{\infty} dt \langle d \rangle(t) e^{iq\omega t}$. Accordingly, the state of the field after the interaction is shifted $|\phi'\rangle = D(\chi)|\phi\rangle = |\alpha + \chi_1\rangle \otimes_{q=2}^N |\chi_q\rangle$. The shift of the coherent state amplitude of the driving laser $\chi_1 = \delta\alpha$ accounts for the depletion of the fundamental mode due to HHG, which modes are displaced by χ_q . However, since the depletion of the fundamental mode and the shift of the harmonic modes are correlated, the actual mode which is excited due to the interaction with the atomic medium is given by a wave packet mode consisting of all field modes participating in the process. The excitation of this wave packet mode can be described by the creation operator B^\dagger , with the corresponding number states $|\tilde{n}\rangle$ satisfying $B^\dagger B|\tilde{n}\rangle = \tilde{n}|\tilde{n}\rangle$. It is this wave packet mode that is excited during the HHG process [30]. In order to take into account

the correlation between the shift of the fundamental and harmonic modes, we represent the total state $|\phi'\rangle$ in terms of the wave packet mode $|\tilde{n}\rangle$. Considering only those cases where an excitation of the wave packet mode is present, but without discriminating between the number of excitation, we project on $\sum_{\tilde{n} \neq 0} |\tilde{n}\rangle\langle\tilde{n}|$, and obtain

$$|\psi\rangle = [1 - \langle\tilde{0}|\langle\tilde{0}|]|\alpha + \delta\alpha\rangle \otimes_{q=2}^N |\chi_q\rangle. \quad (1)$$

Recalling that the vacuum state of this wave packet mode is given by the initial state before the interaction, i.e., $|\tilde{0}\rangle \equiv D(\alpha)|0\rangle \otimes |\{0_q\}\rangle$, the total state of the field after the HHG process is given by (up to normalization)

$$|\psi\rangle = |\alpha + \delta\alpha\rangle \otimes_{q=2}^N |\chi_q\rangle - \langle\alpha|\alpha + \delta\alpha\rangle |\alpha\rangle \otimes_{q=2}^N \langle 0_q|\chi_q\rangle |0_q\rangle. \quad (2)$$

It shows that in the process of HHG all field modes, including the fundamental and all harmonic modes, are naturally entangled. Thus, whenever harmonics are generated the state of the total optical field is entangled. Note that the field modes are entangled in such a way that measuring one mode can leave the entanglement of the other modes intact, which suggests the ability of using HHG for generating high dimensional optical cluster states [39] which are used for measurement based quantum computation [40,41].

This entangled state, which is heralded by the generation of harmonic radiation, shall now be used to generate nonclassical coherent state superposition from the far-IR to XUV spectral region. This is achieved by using the scheme developed in [30] for the generation of optical cat states in the IR regime. This scheme is illustrated in Fig. 1, and relies on a postselection procedure by performing a measurement on the harmonic modes without photon number resolving detectors [30,34]. Part of this

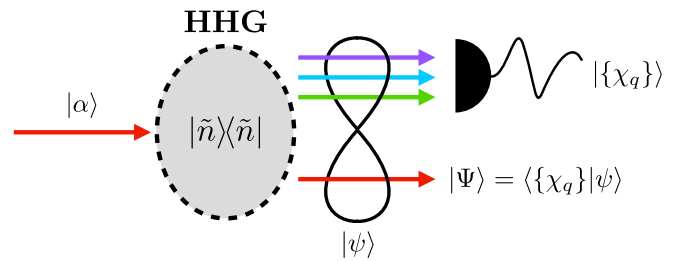


FIG. 1. Schematic illustration of the conditioning measurement performed in HHG to generate coherent state superposition. The intense driving laser in the fundamental mode described by the coherent state $|\alpha\rangle$ interacts with a HHG medium, and the generated optical field is in the wave packet mode corresponding to $|\tilde{n}\rangle$. This gives rise to an entangled state between all field modes $|\psi\rangle$. Performing a conditioning measurement on the harmonic modes, by projecting on $|\{\chi_q\}\rangle = \otimes_q |\chi_q\rangle$, the fundamental mode is found in the coherent state superposition $|\Psi\rangle$.

measurement constitutes a conditioning on HHG by separating it from other processes (like ionization), i.e., taking only into account the wave packet excitations via $|\tilde{n}\rangle$. Thus, the fundamental mode conditioned on the harmonic signal is given by projecting on the harmonic coherent states $|\Psi\rangle = \langle\{\chi_q\}|\psi\rangle$ of amplitude χ_q . The fundamental mode, up to normalization, is then found to be in a superposition of coherent states

$$|\Psi\rangle = |\alpha + \delta\alpha\rangle - \langle\alpha|\alpha + \delta\alpha\rangle e^{-\Omega}|\alpha\rangle, \quad (3)$$

where $\Omega = \sum_{q>1} |\chi_q|^2$. This state coincides with the state recently reported and measured in [30], but with the proper prefactor for the second term which takes into account all modes appearing in the experiment. To understand the influence of the decoherence factor Ω we only consider energy conserving events during HHG, i.e., $|\delta\alpha|^2 = \sum_{q=3}^N q|\chi_q|^2$. Assuming that the shift of the harmonics are equal, and using that in single-color HHG only odd harmonics are generated, we find that $\Omega = 2|\delta\alpha|^2(N-1)/(N^2 + 2N - 3)$. We thus observe that the influence of the harmonics scales as $\mathcal{O}(1/N)$ with the harmonic cutoff. Because of the extension to large harmonic orders, it makes the scheme intrinsically robust against this kind of decoherence [see Supplemental Material [42] (SM) for more details].

However, due to the complete multimode description of the HHG process developed in this work, we can further generalize this scheme to generate nonclassical optical states in extreme wavelength regimes. In fact the process of HHG allows us to generate entanglement between different frequency modes of the optical field ranging from the far-IR to the XUV regime. Depending on the particular modes measured on the state (2), for instance measuring all modes except $\tilde{q} \in \{q_i, q_j\}$, we obtain the entangled state

$$|\Psi_{ij}\rangle = \bigotimes_{\tilde{q}} |\chi_{\tilde{q}}\rangle - e^{-\Omega_{ij}} \bigotimes_{\tilde{q}} \langle 0_{\tilde{q}} | \chi_{\tilde{q}} \rangle |0_{\tilde{q}}\rangle, \quad (4)$$

where $\Omega_{ij} = \sum_{q \neq \tilde{q}} |\chi_{\tilde{q}}|^2$. Note that for the driving laser mode we have $|0_1\rangle \equiv |\alpha\rangle$ and $|\chi_1\rangle \equiv |\alpha + \delta\alpha\rangle$. This scheme therefore leads to entangled states between IR-IR, IR-XUV, and XUV-XUV modes by choosing q_i and q_j appropriately. For instance, by interchanging the role of the fundamental with the harmonics, i.e., measuring the fundamental mode and projecting (2) on the coherent state $|\alpha + \delta\alpha\rangle$, we obtain the entangled state of all harmonic modes

$$|\Psi_{\Omega}\rangle = \bigotimes_q |\chi_q\rangle - e^{-|\delta\alpha|^2} \bigotimes_q e^{-\frac{1}{2}|\chi_q|^2} |0_q\rangle. \quad (5)$$

The fact that the remaining harmonic modes are still entangled, illustrates the peculiar feature of the entangled state in (2) as an optical cluster state with possible

application in quantum information processing. If we further measure the harmonic modes $q' \neq q$, the state of the q th harmonic is given by

$$|\Psi_q\rangle = |\chi_q\rangle - e^{-\gamma} |0_q\rangle, \quad (6)$$

where $\gamma = |\delta\alpha|^2 + \Omega + \frac{1}{2}|\chi_q|^2$ with $\Omega = \sum_{q' \neq q} |\chi_{q'}|^2$. The state $|\Psi_q\rangle$ represents a superposition of a coherent state with the vacuum in the XUV regime. To characterize this state we compute the corresponding Wigner function [43,44]

$$W_q(\beta) = \frac{2N_q^2}{\pi} [e^{-2|\beta - \chi_q|^2} + e^{-(\Omega + \Omega')} e^{-2|\delta\alpha|^2} e^{-2|\beta|^2} - e^{-\Omega} e^{-|\delta\alpha|^2} e^{-2|\beta|^2} (e^{2\beta\chi_q^*} + e^{2\beta^*\chi_q})], \quad (7)$$

with the normalization N_q of (6). In Fig. 2(a) we show the Wigner function (7) for an XUV field of wavelength $\lambda_{\text{XUV}} = 72.7$ nm for the 11th harmonic of a driving laser with frequency $\lambda_{\text{IR}} = 800$ nm. For comparison, Fig. 2(b) shows the Wigner function of the IR field corresponding to (3). The nonclassical features of the XUV and IR coherent state superposition are clearly visible, as both deviate from the Gaussian distribution of a coherent state and depict negative values. Since the corresponding mean photon number for the Wigner functions of Fig. 2(a) is less than one, it makes this scheme an interesting source for generating single XUV photons.

However, to obtain a genuine high photon number coherent state superposition in the XUV regime, a second and independent HHG process can be added to the proposed scheme. In the second HHG process, harmonics are generated within the same frequency mode with amplitude χ'_q . Formally, coherently adding the harmonic mode from both schemes, i.e., the low photon number coherent state superposition (6) with the high photon number coherent state $|\chi'_q\rangle$, gives rise to the coherent state superposition

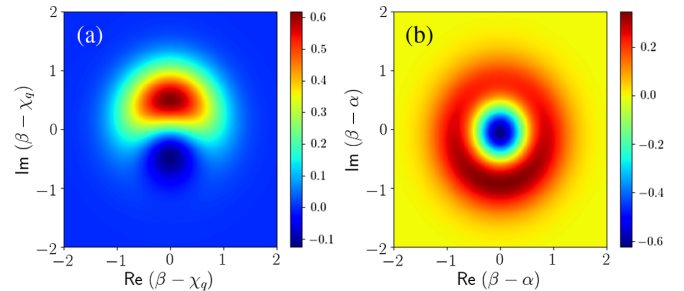


FIG. 2. Wigner function of the coherent state superposition (a) of the q th harmonic Eq. (6) and (b) of the fundamental mode corresponding to Eq. (3). The calculation has been performed using $\delta\alpha = -0.2$, such that $\chi_q \approx 0.03$ for a harmonic cutoff $N = 11$. The opposite shift in imaginary part reflects the correlation between the field modes.

$$|\Psi'_q\rangle = D(\chi'_q)|\Psi_q\rangle = |\chi'_q + \chi_q\rangle - e^{i\phi'} e^{-\gamma} |\chi'_q\rangle, \quad (8)$$

where $\phi' = \text{Im}(\chi'_q \chi_q^*)$. Regardless of the small average photon number in (6) with $\chi_q \ll 1$, the spatiotemporal overlap with the large amplitude coherent state $|\chi'_q\rangle$ leads to the effective displacement operation in (8) [45]. Thus, the coherent state superposition in the IR (3) and XUV (8) describe large amplitude optical cat states. Taking into account the typical photon numbers of the IR driving field and the conversion efficiency of the HHG process [46], the IR and XUV cat state can be produced with photon numbers in the range of $\langle n_{\text{IR}} \rangle \sim 10^{13}$ and $\langle n_{\text{XUV}} \rangle \sim 10^7$ photons per pulse, respectively. Here we want to emphasize that HHG is performed in vacuum such that the optical field is subjected to negligible environmental decoherence effects during propagation. In addition to the technological importance of generating coherent state superpositions in the XUV and IR spectral range, they depict a notable feature which has a direct consequence to fundamental test of quantum theory. Namely, the opposite shift in the imaginary part of their Wigner function is a result of the correlation in the shift of the coherent state amplitudes of the field modes in the process of HHG. Such quantum correlations between field modes can be used, via homodyne quadrature measurements, towards violating Bell-type inequalities [4,5].

However, to generate genuine high photon number entangled coherent states in the order of $|\alpha| = 10^6$ we generalize the HHG process by using a two-color driving field. Such high harmonic generation experiments are often performed for a $\omega - 2\omega$ laser frequency configuration with frequencies in the visible to far-infrared spectral region, with parallel or orthogonal polarizations between the two driving lasers [47–49]. In this case, the initial state of the two mode driving field is given by $|\alpha_1\rangle \otimes |\alpha_2\rangle$, such that the total field after the interaction with the HHG medium is given by $|\alpha_1 + \delta\alpha_1\rangle \otimes |\alpha_2 + \delta\alpha_2\rangle \otimes |\{\bar{\chi}_q\}\rangle$, where $\delta\alpha_1$ and $\delta\alpha_2$ are the depletion of the two driving field modes, respectively. Following the procedure introduced above, and after taking into account the correlations via the corresponding wave packet mode, the obtained state reads

$$|\Psi\rangle = |\alpha_1 + \delta\alpha_1\rangle \otimes |\alpha_2 + \delta\alpha_2\rangle \bigotimes_{q>2} |\bar{\chi}_q\rangle - e^{-i(\varphi_1 + \varphi_2)} e^{-\frac{1}{2}\Delta} |\alpha_1\rangle \otimes |\alpha_2\rangle \bigotimes_{q>2} e^{-\frac{1}{2}|\bar{\chi}_q|^2} |0_q\rangle, \quad (9)$$

where $\varphi_i = \text{Im}(\alpha_i \delta\alpha_i^*)$ and $\Delta = |\delta\alpha_1|^2 + |\delta\alpha_2|^2$. By conditioning on the harmonic signal, i.e., projecting on $|\{\bar{\chi}_q\}\rangle$, we obtain

$$|\text{ECS}\rangle = |\alpha_1 + \delta\alpha_1\rangle \otimes |\alpha_2 + \delta\alpha_2\rangle - e^{-i(\varphi_1 + \varphi_2)} e^{-\frac{1}{2}\Delta} e^{-\bar{\Omega}} |\alpha_1\rangle \otimes |\alpha_2\rangle, \quad (10)$$

with $\bar{\Omega} = \sum_{q>2} |\bar{\chi}_q|^2$. This scheme can be utilized in the spectral range from the visible to the far-infrared regime, which is within the telecom optical fiber wavelength regime useful for long distance entanglement distribution for quantum information processing due to minimized attenuation. Because of the high degree of coherent control in the two-color HHG processes, the relative field amplitudes and phase of the amplitude entangled state between the two physical frequency modes can be tailored in a controllable way. For instance, by independently varying the driving field amplitudes α_i or the relative depletion $\delta\alpha_i$ via the respective field polarization, e.g., linear or circular orthogonal polarized fields.

In order to compare the single- and two-color HHG setup we shall quantify the degree of entanglement between the field modes in each scheme. We will make use of the degree of purity of the reduced density matrix of a subsystem. Since the reduced density matrix of an entangled state is not pure $\rho^2 \neq \rho$, we use the linear entropy $S_{\text{lin}} = 1 - \text{Tr}(\rho^2)$ as a quantitative measure of the involved entanglement between coherent states [50,51]. Since $\text{Tr}(\rho^2) \leq 1$, where the equality only holds for pure states, a nonvanishing linear entropy serves as a witness of entanglement in the total system. For the single-color HHG experiment (2) we particularly focus on two cases. First, on the entanglement between the fundamental driving field with all harmonic modes, and second, on the entanglement of n harmonic modes with all remaining modes (including the fundamental). We thus compute the reduced density matrices of the fundamental mode, and for the $q \in \{2, \dots, n+1\}$ harmonics via $\rho_{q=1} = \text{Tr}_{q>1}(|\psi\rangle\langle\psi|)$, and $\rho_{nq} = \text{Tr}_{q \neq q}(|\psi\rangle\langle\psi|)$, respectively. The corresponding linear entropy measures, for the fundamental mode S_{lin}^1 (black, solid line) and for n harmonics S_{lin}^{nq} (black dashed line and dotted line), are shown in Fig. 3 as a function of $|\delta\alpha|$ (SM) [42]. The entanglement witness depends on the depletion of the fundamental mode $\delta\alpha$, which is correlated to the harmonic amplitude χ_q . We observe that the entanglement between the fundamental mode with the harmonics (solid) is larger than the entanglement between n harmonic modes with all other field modes (dashed, dotted), and that the entanglement measure monotonically decreases for an increasing depletion of the fundamental mode. For large $\delta\alpha$, all entanglement decays since the amplitude of the second term in (2) vanishes due to the decreasing overlap between the two coherent states. For the different partitions of the n harmonic modes we observe that for larger n the entanglement with the remaining modes is increased and almost negligible for $n = 1$. For the two-color HHG process in which an entangled pair of coherent states of large amplitude can be generated (10), we quantify the involved entanglement by tracing over the second 2ω driving field mode in (10). The corresponding linear entropy S'_{lin} is shown in Fig. 3 (red) for different ratios of the depletion of the two modes $r = |\delta\alpha_2|^2 / |\delta\alpha_1|^2$ (SM). We observe that for

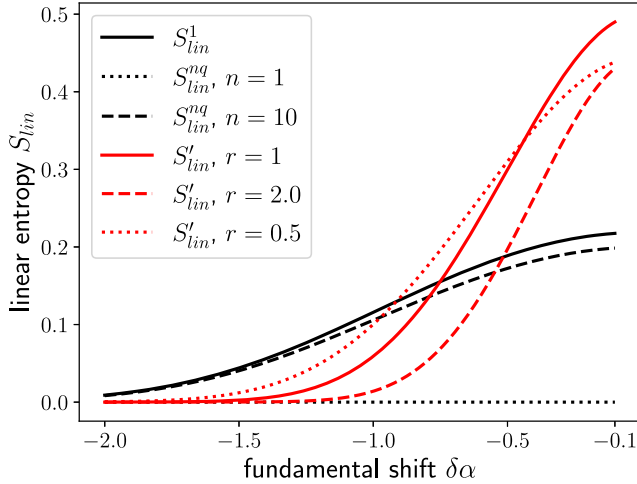


FIG. 3. Linear entropy measures S_{lin}^1 (black solid line) and S_{lin}^{nq} for two different partitions of the entangled state (2) with $n = 1$ (black dashed line) and $n = 10$ (black dotted line) for increasing depletion of the fundamental mode $|\delta\alpha|$. The linear entropy measure for the two-color high harmonic generation experiment S_{lin}^r (red) with different ratios of the depletion of the two driving fields $r = |\delta\alpha_2|^2/|\delta\alpha_1|^2$. In all cases we have used the harmonic cutoff at $N = 11$.

small depletion the involved entanglement between the two driving field modes in the two-color HHG experiment is larger than in any single-color experiment, and is the largest for equal depletion (red, solid line). For a larger depletion $|\delta\alpha|$ the entanglement decays slower when the 2ω field has smaller depletion than the ω mode, e.g., $r = 0.5$ (red, dotted line). In the opposite case, with $r = 2.0$, the entanglement is smallest (red, dashed line).

In conclusion, we developed a quantum mechanical multimode approach for the description of HHG driven by single- and two-color intense laser fields. We showed that all field modes involved in the HHG process are naturally entangled once harmonics are generated. Performing quantum operations on particular field modes leads to the generation of high photon number coherent state superpositions spanning from the XUV to the far IR spectral region. We provided the conditions for the generation of XUV-IR correlated coherent state superposition, and the generation of entangled states in the visible-IR spectral region with controllable quantum features. The entangled states generated by using HHG are deterministically generated whenever harmonic radiation is emitted, and the coherent state superposition is heralded when the conditioning measured is performed. Considering that a similar HHG mechanism underlies a majority of the intense-laser matter interactions [35,52,53], we anticipate that the findings will set the stage for conceiving novel experiments for the generation of a whole family of high photon number nonclassical entangled field states, challenging the quantum state characterization schemes [54], advancing fundamental studies of quantum theory and

providing a new platform for optical quantum technologies [27]. Finally, we note that the dynamics of the HHG process is intrinsically in the attosecond time regime, which further stress the potential impact of the present work on quantum information technologies towards a previously inaccessible time scale, and can further be used for optical signaling and spectroscopy with nonclassical light states [55].

ICFO group acknowledges support from: ERC AdG NOQIA; Agencia Estatal de Investigación (R&D project CEX2019-000910-S, funded by MCIN/AEI/10.13039/501100011033, Plan National FIDEUA PID2019-106901GB-I00, FPI, QUANTERA MAQS PCI2019-111828-2, Proyectos de I+D+I “Retos Colaboración” QUSPIN RTC2019-007196-7); Fundació Cellex; Fundació Mir-Puig; Generalitat de Catalunya through the European Social Fund FEDER and CERCA program (AGAUR Grant No. 2017 SGR 134, QuantumCAT U16-011424, co-funded by ERDF Operational Program of Catalonia 2014-2020); EU Horizon 2020 FET-OPEN OPTologic (Grant No 899794); National Science Centre, Poland (Symfonia Grant No. 2016/20/W/ST4/00314); European Union’s Horizon 2020 research and innovation programme under the Marie-Sklodowska-Curie Grant Agreement No 101029393 (STREDCH) and No 847648 (“La Caixa” Junior Leaders fellowships ID100010434: LCF/BQ/PI19/11690013, LCF/BQ/PI20/11760031, F/BQ/PR20/11770012, LCF/BQ/PR21/11840013). FORTH group acknowledges LASERLAB-EUROPE (H2020-EU.1.4.1.2 Grant No. 871124), FORTH Synergy Grant AgiDA (Grant No. 00133), the EUs H2020 framework programme for research and innovation under the NFFA-Europe-Pilot project (Grant No. 101007417). ELI-ALPS is supported by the European Union and cofinanced by the European Regional Development Fund (GINOP Grant No. 2.3.6-15-2015-00001). P. S. has received funding from the European Union’s Horizon 2020 research and innovation programme under the Marie Skłodowska-Curie Grant Agreement No 847517. J. R.-D. acknowledges support from the Secretaria d’Universitats i Recerca del Departament d’Empresa i Coneixement de la Generalitat de Catalunya, as well as the European Social Fund (L’FSE inverteix en el teu futur) —FEDER. M. F. C. acknowledges the Guangdong Province Science and Technology Major Project (Future functional materials under extreme conditions 212019071820400001). E. P. acknowledges Royal Society funding under URF/R1\211390.

* philipp.stammer@icfo.eu

- [1] E. Schrödinger, Die gegenwärtige situation in der quantenmechanik, *Naturwissenschaften* **23**, 823 (1935).
- [2] C. C. Gerry and P. L. Knight, Quantum superpositions and Schrödinger cat states in quantum optics, *Am. J. Phys.* **65**, 964 (1997).

- [3] A. Ourjoumtsev, H. Jeong, R. Tualle-Brouri, and P. Grangier, Generation of optical Schrödinger cats from photon number states, *Nature (London)* **448**, 784 (2007).
- [4] J. Wenger, M. Hafezi, F. Grosshans, R. Tualle-Brouri, and P. Grangier, Maximal violation of bell inequalities using continuous-variable measurements, *Phys. Rev. A* **67**, 012105 (2003).
- [5] R. García-Patrón, J. Fiurášek, N.J. Cerf, J. Wenger, R. Tualle-Brouri, and Ph. Grangier, Proposal for a Loophole-Free Bell Test Using Homodyne Detection, *Phys. Rev. Lett.* **93**, 130409 (2004).
- [6] B. C. Sanders, Entangled coherent states, *Phys. Rev. A* **45**, 6811 (1992).
- [7] X. Wang and B. C. Sanders, Multipartite entangled coherent states, *Phys. Rev. A* **65**, 012303 (2001).
- [8] A. Gilchrist, K. Nemoto, W.J. Munro, T.C. Ralph, S. Glancy, S.L. Braunstein, and G.J. Milburn, Schrödinger cats and their power for quantum information processing, *J. Opt. B* **6**, S828 (2004).
- [9] A. Ourjoumtsev, R. Tualle-Brouri, Julien Laurat, and P. Grangier, Generating optical schrödinger kittens for quantum information processing, *Science* **312**, 83 (2006).
- [10] B. Vlastakis, G. Kirchmair, Z. Leghtas, S.E. Nigg, L. Frunzio, S.M. Girvin, M. Mirrahimi, M.H. Devoret, and R.J. Schoelkopf, Deterministically encoding quantum information using 100-photon schrödinger cat states, *Science* **342**, 607 (2013).
- [11] P. Jouguet, S. Kunz-Jacques, A. Leverrier, P. Grangier, and E. Diamanti, Experimental demonstration of long-distance continuous-variable quantum key distribution, *Nat. Photonics* **7**, 378 (2013).
- [12] S. Lloyd and S.L. Braunstein, Quantum computation over continuous variables, in *Quantum Information with Continuous Variables* (Springer, New York, 1999), pp. 9–17.
- [13] T.C. Ralph, A. Gilchrist, G.J. Milburn, W.J. Munro, and S. Glancy, Quantum computation with optical coherent states, *Phys. Rev. A* **68**, 042319 (2003).
- [14] J. Joo, W.J. Munro, and T.P. Spiller, Quantum Metrology with Entangled Coherent States, *Phys. Rev. Lett.* **107**, 083601 (2011).
- [15] A. Zavatta, S. Viciani, and M. Bellini, Quantum-to-classical transition with single-photon-added coherent states of light, *Science* **306**, 660 (2004).
- [16] M. Brune, S. Haroche, J.M. Raimond, L. Davidovich, and N. Zagury, Manipulation of photons in a cavity by dispersive atom-field coupling: Quantum-nondemolition measurements and generation of schrödinger catstates, *Phys. Rev. A* **45**, 5193 (1992).
- [17] B. Hacker, S. Welte, S. Daiss, A. Shaikat, S. Ritter, L. Li, and G. Rempe, Deterministic creation of entangled atom–light schrödinger-cat states, *Nat. Photonics* **13**, 110 (2019).
- [18] M. Dakna, T. Anhut, T. Opatrný, L. Knöll, and D.-G. Welsch, Generating schrödinger-cat-like states by means of conditional measurements on a beam splitter, *Phys. Rev. A* **55**, 3184 (1997).
- [19] A.P. Lund, H. Jeong, T.C. Ralph, and M.S. Kim, Conditional production of superpositions of coherent states with inefficient photon detection, *Phys. Rev. A* **70**, 020101(R) (2004).
- [20] M. Takeoka and M. Sasaki, Conditional generation of an arbitrary superposition of coherent states, *Phys. Rev. A* **75**, 064302 (2007).
- [21] J. Fiurášek, Conditional generation of n-photon entangled states of light, *Phys. Rev. A* **65**, 053818 (2002).
- [22] M.A. Nielsen and I. Chuang, *Quantum computation and quantum information* (Cambridge University Press, Cambridge, 2002).
- [23] Y. Aharonov, P.G. Bergmann, and J.L. Lebowitz, Time symmetry in the quantum process of measurement, *Phys. Rev.* **134**, B1410 (1964).
- [24] P. Stammer, State distinguishability under weak measurement and postselection: A unified system and device perspective, *Phys. Rev. A* **102**, 062206 (2020).
- [25] H. Takahashi, K. Wakui, S. Suzuki, M. Takeoka, K. Hayasaka, A. Furusawa, and M. Sasaki, Generation of Large-Amplitude Coherent-State Superposition via Ancilla-Assisted Photon Subtraction, *Phys. Rev. Lett.* **101**, 233605 (2008).
- [26] E.V. Mikheev, A.S. Pugin, D.A. Kuts, S.A. Podoshvedov, and N.B. An, Efficient production of large-size optical schrödinger cat states, *Sci. Rep.* **9**, 14301 (2019).
- [27] I.A. Walmsley, Quantum optics: Science and technology in a new light, *Science* **348**, 525 (2015).
- [28] T. Brabec and F. Krausz, Intense few-cycle laser fields: Frontiers of nonlinear optics, *Rev. Mod. Phys.* **72**, 545 (2000).
- [29] Th. Lamprou, I. Lontos, N.C. Papadakis, and P. Tzallas, A perspective on high photon flux nonclassical light and applications in nonlinear optics, *High Power Laser Sci. Eng.* **8**, E42 (2020).
- [30] M. Lewenstein, M.F. Ciappina, E. Pisanty, J. Rivera-Dean, P. Stammer, Th. Lamprou, and P. Tzallas, Generation of optical schrödinger cat states in intense laser–matter interactions, *Nat. Phys.* **17**, 1104 (2021).
- [31] M. Lewenstein, Ph. Balcou, M. Yu Ivanov, A. Lhuillier, and P.B. Corkum, Theory of high-harmonic generation by low-frequency laser fields, *Phys. Rev. A* **49**, 2117 (1994).
- [32] I.K. Kominis, G. Kolliopoulos, D. Charalambidis, and P. Tzallas, Quantum-optical nature of the recollision process in high-order-harmonic generation, *Phys. Rev. A* **89**, 063827 (2014).
- [33] I.A. Gonoskov, N. Tsatrafyllis, I.K. Kominis, and P. Tzallas, Quantum optical signatures in strong-field laser physics: Infrared photon counting in high-order-harmonic generation, *Sci. Rep.* **6**, 32821 (2016).
- [34] N. Tsatrafyllis, I.K. Kominis, I.A. Gonoskov, and P. Tzallas, High-order harmonics measured by the photon statistics of the infrared driving-field exiting the atomic medium, *Nat. Commun.* **8**, 15170 (2017).
- [35] N. Tsatrafyllis, S. Kühn, M. Dumergue, P. Foldi, S. Kahaly, E. Cormier, I.A. Gonoskov, B. Kiss, K. Varju, S. Varro *et al.*, Quantum Optical Signatures in a Strong Laser Pulse After Interaction with Semiconductors, *Phys. Rev. Lett.* **122**, 193602 (2019).
- [36] A. Gorlach, O. Neufeld, N. Rivera, O. Cohen, and I. Kaminer, The quantum-optical nature of high harmonic generation, *Nat. Commun.* **11**, 4598 (2020).

- [37] B. Sundaram and P.W. Milonni, High-order harmonic generation: Simplified model and relevance of single-atom theories to experiment, *Phys. Rev. A* **41**, 6571 (1990).
- [38] J. Rivera-Dean, T. Lamprou, E. Pisanty, P. Stammer, A. F. Ordóñez, M. F. Ciappina, M. Lewenstein, and Paraskevas Tzallas, Quantum optics of strongly laser-driven atoms and generation of high photon number optical cat states, [arXiv:2110.01032](https://arxiv.org/abs/2110.01032).
- [39] R. Raussendorf and H. J. Briegel, A One-Way Quantum Computer, *Phys. Rev. Lett.* **86**, 5188 (2001).
- [40] D. E. Browne and T. Rudolph, Resource-Efficient Linear Optical Quantum Computation, *Phys. Rev. Lett.* **95**, 010501 (2005).
- [41] P. Walther, K. J. Resch, T. Rudolph, E. Schenck, H. Weinfurter, V. Vedral, M. Aspelmeyer, and A. Zeilinger, Experimental one-way quantum computing, *Nature (London)* **434**, 169 (2005).
- [42] See Supplemental Material at <http://link.aps.org/supplemental/10.1103/PhysRevLett.128.123603> for the derivation of the $\mathcal{O}(1/N)$ scaling law for the decoherence factor in the optical cat state, and an analysis of the influence on the negativity of the corresponding Wigner function. We further provide the exact expressions for the reduced density matrix and linear entropy measure.
- [43] A. Royer, Measurement of quantum states and the wigner function, *Found. Phys.* **19**, 3 (1989).
- [44] J. Rivera-Dean, P. Stammer, E. Pisanty, Th. Lamprou, P. Tzallas, M. Lewenstein, and M. F. Ciappina, New schemes for creating large optical schrödinger cat states using strong laser fields, *J. Comput. Electron.* **20**, 2111 (2021).
- [45] M. G. A. Paris, Displacement operator by beam splitter, *Phys. Lett. A* **217**, 78 (1996).
- [46] S. Chatziathanasiou, S. Kahaly, E. Skantzakis, G. Sansone, R. Lopez-Martens, S. Haessler, K. Varju, G. D. Tsakiris, D. Charalambidis, and P. Tzallas, Generation of attosecond light pulses from gas and solid state media, *Photonics* **4**, 26 (2017).
- [47] I. J. Kim, C. M. Kim, H. T. Kim, G. H. Lee, Y. S. Lee, J. Y. Park, D. J. Cho, and C. H. Nam, Highly Efficient High-Harmonic Generation in an Orthogonally Polarized Two-Color Laser Field, *Phys. Rev. Lett.* **94**, 243901 (2005).
- [48] J. Mauritsson, P. Johnsson, E. Gustafsson, A. L'Huillier, K. J. Schafer, and M. B. Gaarde, Attosecond Pulse Trains Generated Using Two Color Laser Fields, *Phys. Rev. Lett.* **97**, 013001 (2006).
- [49] A. Fleischer, O. Kfir, T. Diskin, P. Sidorenko, and O. Cohen, Spin angular momentum and tunable polarization in high-harmonic generation, *Nat. Photonics* **8**, 543 (2014).
- [50] G. S. Agarwal and A. Biswas, Quantitative measures of entanglement in pair-coherent states, *J. Opt. B* **7**, 350 (2005).
- [51] K. Berrada, S. Abdel-Khalek, Hichem. Eleuch, and Y. Hassouni, Beam splitting and entanglement generation: Excited coherent states, *Quantum Inf. Process.* **12**, 69 (2013).
- [52] E. N. Osika, A. Chacón, L. Ortmann, N. Suárez, J. A. Pérez-Hernández, B. Szafran, M. F. Ciappina, F. Sols, A. S. Landsman, and M. Lewenstein, Wannier-Bloch Approach to Localization in High-Harmonics Generation in Solids, *Phys. Rev. X* **7**, 021017 (2017).
- [53] Th. Lamprou, R. Lopez-Martens, S. Haessler, I. Liontos, S. Kahaly, J. Rivera-Dean, P. Stammer, E. Pisanty, M. F. Ciappina, M. Lewenstein *et al.*, Quantum-optical spectrometry in relativistic laser-plasma interactions using the high-harmonic generation process: A proposal, *Photonics* **8**, 192 (2021).
- [54] S. Fuchs, J. J. Abel, J. Nathanael, J. Reinhard, F. Wiesner, M. Wünsche, S. Skruszewicz, C. Rödel, D. Born, H. Schmidt *et al.*, Photon counting of extreme ultraviolet high harmonics using a superconducting nanowire single-photon detector, *Appl. Phys. B* **128**, 26 (2022).
- [55] K. E. Dorfman, F. Schlawin, and S. Mukamel, Nonlinear optical signals and spectroscopy with quantum light, *Rev. Mod. Phys.* **88**, 045008 (2016).